Published in final edited form as:
J Immunol. 2012 December 15; 189(12): 5924–5933. doi:10.4049/jimmunol.1202322.

On the Role of Regulatory T Cells During Viral Induced Inflammatory Lesions

Tamara Veiga-Parga[*], **Amol Suryawanshi**[†], **Sachin Mulik**[*], **Fernanda Giménez**[*], **Shalini Sharma**[‡], **Tim Sparwasser**[§], and **Barry T Rouse**[*]

[*]Department of Biomedical and Diagnostic Sciences, College of Veterinary Medicine, University of Tennessee, Knoxville, TN, USA

[†]Department of Ophthalmology, Tufts University School of Medicine, Boston, MA 02111

[‡]Department of Immunology, St. Jude Children's Research Hospital, Memphis, TN, 38105-3678

[§]Institute for Infection Immunology, TWINCORE, Feodor-Lynen-Str. 7, 30625 Hannover, Germany

Abstract

Ocular HSV-1 infection can result in SK, a blinding immunoinflammatory lesion that represents an immunopathological response to the infection. $CD4^+$ T cells are the main orchestrators, and lesions are more severe if the regulatory T cell response is compromised from the onset of infection. Little is known about the role for $Foxp3^+$ $CD4^+$ Tregs during ongoing inflammatory reactions, which is the topic of this report. We used DEREG mice and depleted Treg at different times after infection. We show that lesions became more severe even when depletion was begun in the clinical phase of the disease. This outcome was explained both by Treg influencing the activity of inflammatory effector T cells at the lesion site, as well as an effect in lymphoid tissues that led to reduced numbers of effectors and less trafficking of T cells and neutrophils to the eye. Our results demonstrate that Treg can beneficially influence the impact of ongoing tissue damaging responses to a virus infection and imply that therapies that boost Treg function in the clinical phase hold promise as a modality to control a lesion that is an important cause of human blindness.

Introduction

Ocular infection with HSV-1 can result in a chronic immunoinflammatory lesion in the corneal stroma, which is a significant cause of human vision loss (1, 2). Studies in animal models have revealed that SK lesions are orchestrated mainly by IFN-γ producing $CD4^+$ T cells (Th1) (3, 4) and to a lesser extent by IL-17 producing $CD4^+$ T cells (Th17) (5). Lesion severity is also subject to modulation by several host derived factors, which include IL-10 (6), some galectins (7, 8), microRNAs (9), as well as by Treg (10, 11). Thus removing or expanding Treg from the onset of lesion induction results in exacerbated or diminished lesions, respectively (10, 12). The role for Treg in modulating lesion severity in multiple autoimmune diseases is well established (13, 14), and Treg are suspected to play a similar role in several chronic infections, which include hepatitis C and some of the lesions caused by HIV (15, 16). However, few if any studies have evaluated the role of Treg in an infection-induced lesion by removing them during the ongoing disease process. A recent study did perform such a study removing Treg several days after intracerebral infection with

Address correspondence and reprint requests to Dr. Barry T. Rouse, Department of Biomedical and Diagnostic Sciences, College of Veterinary Medicine, 1414 Cumberland Avenue, Rm. F403, Knoxville, TN 37996, USA. btr@utk.edu.

measles virus (17). They showed that viral clearance was accelerated, but did not evaluate any changes in tissue damage.

In the present report, we have evaluated the lesion modulating consequences of Treg removal after lesions have commenced in a system where tissue damage is caused by an immunopathological response to infection. Our results show that Treg depletion resulted in increased lesion severity with the effect less evident as the depletion was delayed further from the time of infection. The consequences of Treg removal appeared to have two explanations. These were inhibitory effects at the lesion site, as well as effects in lymphoid tissues that reduced the migration of inflammatory cells to the tissue lesion. Our results indicate that Treg play a beneficial role to minimize and modulate the severity of viral-induced immuno-inflammatory reactions. This could mean that expanding Treg function could represent a promising approach for therapy.

Materials and Methods

Ethics statement

This study was carried out in strict accordance with the recommendations in the Guide for the Care and Use of Laboratory Animals of the National Research Council. All animals were housed in Association for Assessment and Accreditation of Laboratory Animal Care (AAALAC)-approved animal facilities. The protocol was approved by the Institutional Animal Care and Use Committee of the University of Tennessee (PHS Assurance number A3668-01). HSV-1 eye infection was performed under deep anesthesia (avertin), and all efforts were made to minimize animal suffering.

Mice, virus, and cell lines

Breeder pairs of DEREG mice on C57BL/6 background were provided by Dr. Tim Sparwasser (Munich, Germany), and additional mice were bred in the Walters Life Sciences animal facility at the University of Tennessee, Knoxville. For the experiments, female 5 to 6 weeks old were used. All manipulations were done in a laminar flow hood. All experimental procedures were in complete agreement with the Association for Research in Vision and Ophthalmology resolution on the use of animals in research. HSV-1 RE, originally provided by the Robert N. Lausch laboratory, was used in all procedures. Virus was grown and titrated on Vero cells (American Type Culture Collection no. CCL81) using standard protocols. The virus was stored in aliquots at − 80°C until use.

Abs

CD4-allophycocyanin (RM4.5), CD4-Percp (RM4.5), CD103-allophycocyanin (2E7), CTLA-4-PE (UC10-4F10-11), CD45-allophycocyanin (30-F11), CD11b-PerCP (M1/70), Ly6G-PE (1A8), CD49d-PE (MFR4.B), CD44-Percp (IM7), and IFN-γ-allophycocyanin (XMG1.2) were purchased from BD Biosciences; ICOS-PE (7E.17G9), PD1-PE (J43), F4/80-PE (BM8), CD62L-Percp (MEL-14) were purchased from eBioscience.

Corneal HSV-1 infection and clinical observations

Corneal infections of C57BL/6 mice were done under deep anesthesia induced by intra-peritoneal injection in tribromoethanol (avertin) as previously described (18). Corneas were scarified with a 27-gauge needle, and a 3-μl drop containing the specific viral dose (2×10^3 PFU) was applied to the eye. Eyes were examined on different days p.i. with a slit-lamp biomicroscope (Kowa Company, Nagoya, Japan) measuring the progression of SK lesion severity and angiogenesis of individual mice. The scoring system was as follows: 0, normal cornea; +1, mild corneal haze; +2, moderate corneal opacity or scarring; +3, severe corneal opacity but iris visible; +4, opaque cornea and corneal ulcer; +5, corneal rupture and

necrotizing keratitis (19). The severity of angiogenesis was recorded as described previously (20). According to this system, a grade of 4 for a given quadrant of the circle represents a centripetal growth of 1.5 mm toward the corneal center. The score of the four quadrants of the eye were then summed to derive the neovessel index (range 0-16) for each eye at a given time point.

Depletion of Treg

To deplete Treg cells, DEREG mice were injected with DT (from *Corynebacterium diphtheriae,* Sigma). Mice were injected intra-peritoneally with 1 μg DT every other day. Control mice were DEREG mice injected with the vehicle.

Histopathology

Eyes from control and DT-treated mice starting on day 8 p.i. were extirpated on day 15 p.i. and snap frozen in OCT compound (Miles, Elkart, IN). Six-micron-thick sections were cut and air dried in a desiccation box. Staining was performed with hematoxylin and eosin (Richard Allen Scientific, Kalamazoo, MI).

Flow cytometry

Cell preparation—Single cell suspensions were prepared from cornea, cervical DLNs, and spleen of mice at different time points p.i. Corneas were excised, pooled group wise, and digested with 60 U/ml Liberase (Roche Diagnostics) for 35 min at 37°C in a humified atmosphere of 5% CO_2. After incubation, the corneas were disrupted by grinding with a syringe plunger on a cell strainer, and a single-cell suspension was made in complete RPMI 1640 medium.

Staining for flow cytometry—The single cell suspensions obtained from corneas, DLNs, and spleen were stained for different cell surface molecules for FACS. All steps were performed at 4°C. A total of 1×10^6 cells were first blocked with an unconjugated anti-CD32/CD16 mAb for 30 min in FACS buffer. After washing with FACS buffer, fluorochrome-labeled respective antibodies were added for 30 min on ice. Finally, the cells were washed three times and re-suspended in 1% *para*-formaldehyde. The stained samples were acquired with a FACS Calibur (BD Biosciences), and the data were analyzed using FlowJo software. For corneas, total cell numbers were calculated by acquiring the totality of the sample and taking into consideration total number of corneas in the sample.

To enumerate the number of IFN-γ-producing $CD4^+$ T cells, intracellular cytokine staining was performed as previously described (21). In brief, 10^6 freshly isolated splenocytes, and lymph node and corneal cells were cultured in U-bottom 96-well plates. For *in vitro* induced cultures, cells were left unstimulated or stimulated with PMA (50 ng) and ionomycin (500 ng) for 4 h in the presence of brefeldin A (10 μg/ml). Subsequently, cell surface staining was performed, followed by intracellular cytokine staining using a Cytofix/Cytoperm kit (BD Pharmingen) in accordance with the manufacturer's recommendations. The Abs used were anti-IFN-γ allophycocyanin. The fixed cells were resuspended in 1% paraformaldehyde. The stained samples were acquired with a FACS Calibur (BD biosciences), and the data were analyzed using FlowJo software. For intracellular staining of CTLA-4, we used Foxp3 Staining Buffer Set (eBioscience).

Real-time PCR

RNA was extracted from cells and tissue using TRIzol LS reagent (Invitrogen). Total cDNA was made with 500 ng of RNA using oligo(dT) primer. Q-RT-PCR was performed using SYBR Green PCR Master Mix (Applied Biosystems, Foster City, CA) with an iQ5 RT-PCR

detection system (Bio Rad, Hercules, CA) using 5 μl cDNA for 40 cycles. The expression levels of different molecules were normalized to β-actin using the Δ threshold cycle method calculation. Relative expression between mock-infected samples and control or day 8 DT-treated samples from day 15 p.i. were calculated using the $2^{-\Delta\Delta Ct}$ formula: $\Delta\Delta Ct = \Delta Ct_{sample} - \Delta Ct_{reference}$. Here, ΔCt is the change in cycling threshold between the gene of interest and the "housekeeping" gene β-actin, where ΔCt_{sample} was the Ct value for any day 8 DT-treated or control samples from day 15 p.i. normalized to the β-actin gene, and $\Delta Ct_{reference}$ was the Ct value for the mock-infected samples (scratched and infected only with PBS) also normalized to β-actin. Each of the samples was run in duplicate to determine sample reproducibility, and a mean Ct value for each duplicate measurement was calculated. The PCR primers used were the following: βactin, F 5′-CCTTCTTGGGTATGGAATCCTG-3′ and R 5′-GGCATAGAGGTCTTTACGGATG-3′; IL-6, F 5′-CGTGGAAATGAGAAAAGAGTTGTGC-3′ and R 5′-ATGCTTAGGCATAACGCACTAGGT-3′; IL-1β, F 5′-GAAATGCCACCTTTTGACAG-3′ and R 5′-CAAGGCCACAGGTATTTTGT-3′; IFN-γ, F 5′-GGATGCATTCATGAGTATTGC-3′ and R 5′-GCTTCCTGAGGCTGGATTC-3′; CXCL-9, F 5′-CAAGCCCCAATTGCAACAAA-3′ and R 5′-TCCGGATCTAGGCAGGTTTGA-3′; CXCL-10, F 5′-TGCTGGGTCTGAAGTGGGACT-3′ and R 5′-AAG CTT CCC TAT GGC CCT CA-3′; MCP-1/CCL2, F 5′-TGGCTCAGCCAGATGCAGT-3′ and R 5′-TTGGGATCATCTTGCTGGTG-3′; KC/CXCL1, F 5′-GTGTTGCCCTCAGGGCC-3′ and R 5′-GCCTCGCGACCATTCTTG-3′.

ELISA

DLN single cell suspensions from individual mice were collected at day 15 p.i. Cells were stimulated in vitro with anti-CD3 (2 μg/ml) and anti-CD28 (1 μg/ml) for 48 h at 37°C. Additionally, corneal samples were pooled groupwise (five corneas per sample) and homogenized using a tissue homogenizer (Pellet Pestle mortar; Kontes). For lymph node samples, four cervical DNLs were collected for each mouse sample, and ELISA was performed on the homogenized sample. The concentrations of IFN-γ were measured by sandwich ELISA kits from eBioscience as per the manufacturers' instructions. *Statistical analysis* Most of the analyses for determining the level of significance were performed using unpaired two-tailed Student *t* tests. Values $***p \leq 0.001$,$**p \leq 0.01$,$*p \leq 0.05$ were considered significant. Results are expressed as means ± SEM. For some experiments, as mentioned in the figure legends, a one-way ANOVA test was applied.

Results

Lymphoid Treg and Th1 response changes after HSV-1 infection

Although previous studies reported that local infection with HSV results in expansion of the Treg population in infected tissues and the lymphoid sites (22), the kinetics of the response was not examined after corneal infection. As shown in Fig. 1A, corneal infection of Foxp3-GFP reporter mice, which express GFP knocked into the locus encoding the transcription factor Foxp3 uniquely expressed by Treg (23), caused expansion of Treg in the DLN as soon as day 4 p.i. Peak numbers were evident by day 8 p.i., when the expansion was approximately 4 fold. Numbers of Th1 cells also peaked on day 8 p.i. (Fig. 1B). The phenotype of Treg was also measured and compared to uninfected controls in the DLN and spleen samples at different time points p.i. (day 0, 4, 8, 12, and 15). As is evident, a greater proportion of Treg from infected animals showed increased expression of activation markers, and more were $CD103^+$ than uninfected controls (Fig. 2A). The expression of other activation markers and costimulatory molecules was also altered after infection (Fig. 2B). The frequency of Treg expressing CTLA-4 and the ICOS significantly increased in DLN

and spleen, peaking on day 15 and day 12 p.i., respectively. The expression of the inhibitory receptor PD-1 also changed, being downregulated after infection until day 8 p.i. and then increasing at later time points (day 12 and 15 p.i.) in both organs. Thus, Treg after HSV-1 infection increase in numbers in lymphoid tissues and change their surface phenotype to a more increased activation phenotype.

Treg depletion increases lesion severity

To measure the outcome of Treg depletion, DEREG animals (a mouse model in which the administration of DT leads to specific depletion of Treg due to expression of DT receptor-enhanced GFP under the control of the Foxp3 promoter (24)) were infected ocularly with HSV and depletion begun either on day 5, 8, or 12 p.i. by administering DT and treating every other day after the starting time. All treatment procedures resulted in almost total depletion of Treg in the cornea and lymphoid tissues when tested at day 15 p.i. (Fig. 3A). Moreover, DT treatment did not affect other lymphocyte subsets (data not shown) when started at all three time points. The consequence of Treg depletion was significantly increased severity of SK lesions (Fig. 3B and C). Moreover, the average time that lesions first became measurable was 1 to 2 days earlier in Treg-depleted compared to control animals. The clinical consequence of Treg depletion was greater in magnitude the earlier the depletion was commenced, although the differences in outcome on day 15 p.i. between animals treated on day 5 and day 8 p.i. were minimal. On the other hand, SK scores from animals that started depletion on day 12 p.i. were increased, but these changes were not statistically significant. The histological findings in corneas showed more severe inflammatory reactions in animals depleted from day 8 p.i. compared to vehicle-treated controls (Fig. 3D). In conclusion, depletion of Treg during the clinical stages of SK resulted in significantly increased lesion severity indicating that Treg play a modulating role during the immunopathological process.

Inflammatory consequences of Treg depletion in the clinical phase of SK

In experiments where depletion was commenced on day 8 p.i., pools of corneas were collected on day 15 p.i. from DT-treated and control animals either to recover inflammatory cells by collagenase digestion or to prepare samples for analysis by Q-RT-PCR) or protein measurement by ELISA. The numbers of $CD45^+$ cells on day 15p.i. were around 3-fold greater in Treg-depleted animals than controls (Fig. 4A). $CD4^+$ T cell numbers, too, were around 3-fold greater in Treg-depleted mice when compared to controls (Fig. 4B). Additionally, the numbers of neutrophils ($CD45^+CD11b^+Ly6G^+$) and macrophages ($CD45^+CD11b^+F4/80^+$) were also significantly greater in Treg-depleted animals compared to control mice (Fig. 4C and 4D).

Experiments of the same design were conducted to compare the effector functions of infiltrated ocular $CD4^+$ T cells in the non-depleted and Treg-depleted DEREG mice. The cells isolated from corneal tissues were stimulated with PMA/ionomycin in the presence of golgi plug for 4 h. The numbers of Th1 cells were increased around 2-fold in the Treg-depleted group compared to control animals (Fig. 4E). The effect of Treg depletion on levels of chemokines present in corneas was also measured either by Q-RT-PCR or proteins by ELISA. As shown in Fig. 5A, samples from depleted animals showed increased levels of molecules known from previous studies to participate in the pathogenesis of SK (25). These included IL-6 and IL-1β that were increased 5 and 13 fold respectively. Additionally, significantly increased levels of chemokines involved in neutrophil (KC) and monocyte (MCP-1) migration, as well as lymphocyte migration (CXCL-9 and CXCL-10), were noted (Fig. 5B). IFN-γ protein levels were also increased approximately 2 fold in Treg depleted mice (Fig. 5C).

The increase in $CD4^+$ T effector cells in Treg-depleted corneas was attributed to an increase in proinflammatory chemokines in the corneas that recruited the inflammatory cells. Another possible explanation could be that Treg control the number of effector T cells generated in lymphoid tissues, making fewer available to enter the inflamed tissues. To assess this possibility, DLN and spleen cells from day 8 p.i. depleted and control animals were compared for the number of Th1 cells on day 15 p.i. The results shown in Fig. 6A-B demonstrate that Th1 cell total numbers in both DLN and spleen were significantly increased in DT recipients when compared to controls. In another set of experiments, DLN extracts were collected on day 15 from control and Treg depleted mice, and samples analyzed by ELISA for IFN-γ protein levels. The data show that Treg depletion increased the production of IFN-γ by almost 2 fold in the depleted mice (Fig. 6C).

Taken together, our results show that Treg depletion during the clinical phase of the disease caused a significant increase in the total cellular infiltration of $Foxp3^-$ $CD4^+$ T cells, neutrophils, and macrophages, as well as the amount of proinflammatory cytokines and chemokines in the corneas of HSV-1 infected mice. Additionally, effector cell numbers and products in lymphoid tissues were increased in the absence of Treg. We interpret these data to mean that Treg normally act to modulate the extent of inflammatory cell molecule production at the tissue site. The Treg also influence Th1 cell numbers and responses in secondary lymphoid tissues, which would reduce the number of cells available to infiltrate the inflamed cornea. Additionally, Treg might act to inhibit the recruitment of inflammatory cells to the tissue site. Some evidence for this effect is described in the next section.

Consequences of Treg depletion on phenotype of effectors in secondary lymphoid tissue

To measure the putative effects of Treg on inflammatory cell recruitment DLN cell populations from day 8 p.i., depleted and control animals were compared for surface expression of molecules considered as involved in tissue migration. Mice were sacrificed 2 days after depletion (day 10) and the phenotype of $CD4^+$ T cells isolated from DLN and spleen evaluated. The expression of the integrin CD49d (a subunit of VLA 4), a molecule known to be involved in the migration of cells to the ocular lesion site (26, 27), on $Foxp3^-CD4^+$ lymphocytes was upregulated from 10% (control) to 15% (depleted) in DLN and from 18% to 32%, respectively, in the spleen. The number of T effectors expressing CD49d was increased 2 fold in DLN and about 2.5 fold in spleen (Fig. 7A). FACS analysis also revealed that removal of Treg on day 8 p.i. enhanced the expression of activation markers on $Foxp3^-$ $CD4^+$ T cells in DLN and spleen. As shown in Fig. 7B, the frequencies of $CD4^+$ T cells expressing $CD44^{hi}$ in the DLN and spleen significantly increased in the Treg-depleted group compared to controls. Furthermore, around 35% of cells in the DLN and 55% in the spleen were $CD62L^{low}$ in the Treg-depleted group compared to 28% and 35%, respectively, in control mice (Fig. 7C). The upregulation of CD49d on $CD4^+$ T cells is likely relevant, since previous studies indicate that blocking CD49d reduces SK (26, 27). Our results are consistent with the possibility that Treg normally act within lymphoid tissues to reduce the expression of surface molecules such as CD49d on activated cells that permit them to migrate to the tissue site. This could mean that effector cells could traffic more effectively to tissue sites when not controlled by Treg during clinical stages of the disease.

Discussion

Many studies have demonstrated that the extent of inflammatory responses is affected by the balance between proinflammatory effectors and events that regulate them, such as the activity of Foxp3 Treg cells (11, 13, 28). The conclusion that Treg play a modulatory role comes largely from studies that compare the outcome in normal animals to that where the Treg composition is manipulated from before or early in the disease process. In this investigation, we asked if Treg play an active modulatory role during the clinical expression

of lesions. This was accomplished by taking advantage of DEREG mice where Treg can be successfully and rapidly removed by exposure to DT, which depletes the $Foxp3^+$ cells because they express the DT receptor (24, 29). We show, using a model in which an inflammatory lesion occurs in the cornea after HSV infection, that lesions became more severe even when depletion was begun in the clinical phase of the disease. This outcome was explained both by Treg influencing the activity of inflammatory effector T cells at the lesion site as well as an effect in lymphoid tissues that led to reduced numbers of effectors and less trafficking of T cells and neutrophils to the eye. Our results demonstrate that Treg can beneficially influence the impact of ongoing tissue damaging responses to a virus infection and imply that therapies that boost Treg function in the clinical phase hold promise as a modality to control a lesion that is an important cause of human blindness.

Since the milestone report from Belkaid and colleagues (30), we have known that Treg are induced by infections and that they play a significant role in shaping the pattern of disease responses. Treg for instance are considered to influence the outcome of persistent infections as they similarly do in autoimmune diseases (13, 15). However, the majority of studies that implicate Treg during an infectious disease either compared the outcome of disease in animals depleted of Treg from the onset with controls, or observed the consequence of boosting Treg responses early or before infection (11, 31, 32). In our study, we attempted to evaluate the function of Treg during an ongoing inflammatory process by removing them when clinical lesions are already present. This was shown by exploiting the transgenic mouse system developed by Sparwasser and colleagues (29) that permits rapid and almost total selective elimination of $Foxp3^+$ Treg at any stage in the disease process. Our results clearly show that removing Treg in the clinical phase of the disease resulted in lesions becoming more severe. This could be demonstrated not only clinically, but also by comparing the number of inflammatory cells and their products in the corneas of Treg-depleted with control animals. In the absence of Treg, greater numbers of the effector T cells that orchestrate lesions were present, as well as non-lymphoid inflammatory cells such as neutrophils, the latter mainly responsible for damage to the corneal stroma (33, 34). Although our results demonstrate that without Treg, lesions became more severe, we provide no direct evidence that the Treg subserve their function only at the tissue site.

The problem with attempts to conclude that Treg exert functional effects solely within inflammatory reactions is that the depletion procedure also had proinflammatory consequences in lymphoid tissues. Accordingly, effector cell numbers were increased by Treg ablation, and the average phenotype of $CD4^+$ T cells involved in orchestrating SK lesions showed changes. These included increased numbers of cells with an activation phenotype and increased cell numbers that expressed molecules shown in previous studies to be required for migration to the corneal tissue site (26). Consequently, it remains possible that the major influence of Treg during the infection occurs by the DLN acting to limit the number of activated T effectors and the generation of inflammatory cells that express receptors that permit their passage to tissue sites. Further experiments are needed to define the relative importance of tissue acting versus lymphoid organ effects of Treg on the inflammatory response. However, as reviewed by Shevach (35), Treg suppress immune responses at multiple levels with different mechanisms of action in different experimental models.

Our observation adds further evidence to the notion that Treg can play a critical role during responses to infections and implies that amplifying their function in the phase of active lesions would likely be beneficial to the outcome. This may be especially relevant in situations such as SK where replicating virus is minimal or absent at the phase of the inflammatory response (25). However, it remains to be shown how the latter effect can be most effectively achieved particularly if, as has been advocated (36), the Treg that function

most effectively need to be antigen specific. In the case of the virus-induced immunopathology caused by HSV ocular infection, Treg may not need to be virus-specific as long as they express the activation and migration phenotypes that permit them to access the site of inflammation (12). Whereas antigen specificity may facilitate the regulatory activity of Treg, it is also conceivable that as long as the Treg are activated and can successfully gain entrance into inflammatory sites, Treg of multiple specificities could still subserve a useful function. This is to be expected, especially when Treg function by producing soluble anti-inflammatory mediators such as IL-10 and TGF-β, and IL35 (35, 36, 37). In addition, in past studies we have shown that the adoptive transfer of $Foxp3^+$ Treg reactive with OVA peptide, can readily enter the inflamed cornea (12). Moreover, there is some evidence that SK lesions may be in part autoreactive (38), meaning that self-reactive Treg, a major fraction of the $Foxp3^+$ Treg population (13, 36), could participate in regulatory lesion severity.

Our study shows that Treg function is needed to limit the extent of virus-induced inflammatory lesions, and implies that expanding and activating Treg could be therapeutically valuable. Moreover, if, as we advocate, Treg do not need to share antigen reactivity with the proinflammatory effectors they regulate, approaches that expand Treg polyclonally are more available than are maneuvers to expand Ag-specific Treg. Of the polyclonal approaches reported, the ones described by Sprent et al (39, 40) and Podack and colleagues (41, 42) have particular appeal. Podack's approach exploits the fact that among naïve and resting T cells, the monoclonal antibody for the TNF receptor 25 (mAbT25) is expressed predominantly on $Foxp3^+$ Treg (41). Moreover, if the receptor is engaged with an agonistic monoclonal antibody, the Treg population is preferentially expanded and activated. We have found this approach to be effective to expand Treg and diminish SK lesions (42). However, the downside of using mAbT25 is that activated effectors also express TNFR25 and may also be expanded, which could lead to and cause exacerbated tissue damage. Fortunately, this problem can be overcome by the coadministration of additional therapies that selectively cause apoptosis of effectors (42).

In conclusion, our results indicate that Treg play a beneficial role to minimize and modulate the severity of SK lesions during the clinical phase. Our results imply that therapies that boost Treg function in the clinical phase hold promise as a modality to control a lesion that is an important cause of human blindness.

Acknowledgments

We thank Dr. John Dunlop, Naveen K. Rajasagi, Pradeep B. J. Reddy, Sid Bhela, Leon Richardson, Misty Bailey and Martin Nuñez for assistance during research and manuscript preparation.

This study was supported by National Institute of Allergy and Infectious Diseases Grant AI 06335 and National Institutes of Health Grant EY 005093.

Abbreviations used in this article:

DNL	draining lymph node
DT	diptheria toxin
Foxp3	forkhead box P3
p.i.	post infection
Q-RT-PCR	quantitative RT-PCR
SK	stromal keratitis

Treg	regulatory T cells

References

1. Pepose, JD. Herpes simplex virus disease: Anterior segment of the eye. In: Pepose, JS.; Holland, GN.; Whlhelmus, KR., editors. Ocular Infection and Immunity. Vol. 27. Mosby, St.; Louis, MO: 1996. p. 905-932.
2. Giménez F, Suryawanshi A, Rouse BT. Pathogenesis of herpes stromal keratitis- A focus on corneal neovascularization. Prog. Retin. Eye Res. 2012 doi:10.1016/jpreteyeres.2012.07.002.
3. Niemialtowski MG, Rouse BT. Predominance of Th1 cells in ocular tissues during herpetic stromal keratitis. J. Immunol. 1992; 149:3035–3039. [PubMed: 1357034]
4. Hendricks RL, Tumpey TM, Finnegan A. IFN-gamma and IL-2 are protective in the skin but pathologic in the corneas of HSV-1-infected mice. J. Immunol. 1992; 149:3023–3028. [PubMed: 1401927]
5. Suryawanshi A, Veiga-Parga T, Rajasagi NK, Reddy PB, Sehrawat S, Sharma S, Rouse BT. Role of IL-17 and Th17 cells in herpes simplex virus-induced corneal immunopathology. J. Immunol. 2011; 187:1919–1930. [PubMed: 21765013]
6. Sarangi PP, Sehrawat S, Suvas S, Rouse BT. IL-10 and natural regulatory T cells: two independent anti-inflammatory mechanisms in herpes simplex virus-induced ocular immunopathology. J. Immunol. 2008; 180:6297–6306. [PubMed: 18424753]
7. Rajasagi NK, Suryawanshi A, Sehrawat S, Reddy PB, Mulik S, Hirashima M, Rouse BT. Galectin-1 reduces the severity of herpes simplex virus-induced ocular immunopathological lesions. J. Immunol. 2012; 188:4631–4643. [PubMed: 22467659]
8. Sehrawat S, Suryawanshi A, Hirashima M, Rouse BT. Role of Tim-3/galectin-9 inhibitory interaction in viral-induced immunopathology: shifting the balance toward regulators. J. Immunol. 2009; 182:3191–3201. [PubMed: 19234217]
9. Mulik S, Xu J, Reddy PB, Rajasagi NK, Gimenez F, Sharma S, Lu PY, Rouse BT. Role of miR-132 in Angiogenesis after Ocular Infection with Herpes Simplex Virus. Am. J. Pathol. 2012; 181:525–534. [PubMed: 22659469]
10. Suvas S, Azkur AK, Kim BS, Kumaraguru U, Rouse BT. CD4+CD25+ regulatory T cells control the severity of viral immunoinflammatory lesions. J. Immunol. 2004; 172:4123–4132. [PubMed: 15034024]
11. Belkaid Y, Rouse BT. Natural regulatory T cells in infectious disease. Nat. Immunol. 2005; 6:353–360. [PubMed: 15785761]
12. Sehrawat S, Suvas S, Sarangi PP, Suryawanshi A, Rouse BT. In vitro-generated antigen-specific CD4+ CD25+ Foxp3+ regulatory T cells control the severity of herpes simplex virus-induced ocular immunoinflammatory lesions. J. Virol. 2008; 82:6838–6851. [PubMed: 18480441]
13. Sakaguchi S, Ono M, Setoguchi R, Yagi H, Hori S, Fehervari Z, Shimizu J, Takahashi T, Nomura T. Foxp3+ CD25+ CD4+ natural regulatory T cells in dominant self-tolerance and autoimmune disease. Immunol. Rev. 2006; 212:8–27. [PubMed: 16903903]
14. Tang Q, Bluestone JA. Regulatory T-cell physiology and application to treat autoimmunity. Immunol. Rev. 2006; 212:217–237. [PubMed: 16903917]
15. Belkaid Y, Tarbell K. Regulatory T cells in the control of host-microorganism interactions. Annu. Rev. Immunol. 2009; 27:551–589. [PubMed: 19302048]
16. Sehrawat S, Rouse BT. Tregs and infections: on the potential value of modifying their function. J. Leukoc. Biol. 2011; 90:1079–1087. [PubMed: 21914856]
17. Reuter D, Sparwasser T, Hünig T, Schneider-Schaulies J. Foxp3+ regulatory T cells control persistence of viral CNS infection. PLoS One. 2012; 7:e33989. [PubMed: 22448284]
18. Zheng M, Deshpande S, Lee S, Ferrara N, Rouse BT. Contribution of vascular endothelial growth factor in the neovascularization process during the pathogenesis of herpetic stromal keratitis. J. Virol. 2001; 75:9828–9835. [PubMed: 11559816]

19. Suryawanshi A, Mulik S, Sharma S, Reddy PB, Sehrawat S, Rouse BT. Ocular neovascularization caused by herpes simplex virus type 1 infection results from breakdown of binding between vascular endothelial growth factor A and its soluble receptor. J. Immunol. 2011; 186:3653–3665. [PubMed: 21325621]
20. Dana MR, Zhu SN, Yamada J. Topical modulation of interleukin-1 activity in corneal neovascularization. Cornea. 1998; 17:403–409. [PubMed: 9676913]
21. Veiga-Parga T, Suryawanshi A, Rouse BT. Controlling viral immunoinflammatory lesions by modulating aryl hydrocarbon receptor signaling. PLoS Pathog. 2011; 7:e1002427. [PubMed: 22174686]
22. Suvas S, Kumaraguru U, Pack CD, Lee S, Rouse BT. CD4+CD25+ T cells regulate virus-specific primary and memory CD8+ T cell responses. J. Exp. Med. 2003; 198:889–901. [PubMed: 12975455]
23. Fontenot JD, Rasmussen JP, Williams LM, Dooley JL, Farr AG, Rudensky AY. Regulatory T cell lineage specification by the forkhead transcription factor foxp3. Immunity. 2005; 22:329–341. [PubMed: 15780990]
24. Kim J, Lahl K, Hori S, Loddenkemper C, Chaudhry A, deRoos P, Rudensky A, Sparwasser T. Cutting edge: depletion of Foxp3+ cells leads to induction of autoimmunity by specific ablation of regulatory T cells in genetically targeted mice. J. Immunol. 2009; 183:7631–7634. [PubMed: 19923467]
25. Biswas PS, Rouse BT. Early events in HSV keratitis--setting the stage for a blinding disease. Microbes Infect. 2005; 7:799–810. [PubMed: 15857807]
26. Zhang X, Jiang S, Manczak M, Sugden B, Adamus G. Phenotypes of T cells infiltrating the eyes in autoimmune anterior uveitis associated with EAE. Invest. Ophthalmol. Vis. Sci. 2002; 43:1499–1508. [PubMed: 11980866]
27. Devine L, Lightman SL, Greenwood J. Role of LFA-1, ICAM-1, VLA-4 and VCAM-1 in lymphocyte migration across retinal pigment epithelial monolayers in vitro. Immunology. 1996; 88:456–462. [PubMed: 8774365]
28. Rouse BT, Sehrawat S. Immunity and immunopathology to viruses: what decides the outcome? Nat. Rev. Immunol. 2010; 10:514–526. [PubMed: 20577268]
29. Lahl K, Loddenkemper C, Drouin C, Freyer J, Arnason J, Eberl G, Hamann A, Wagner H, Huehn J, Sparwasser T. Selective depletion of Foxp3+ regulatory T cells induces a scurfy-like disease. J. Exp. Med. 2007; 204:57–63. [PubMed: 17200412]
30. Belkaid Y, Piccirillo CA, Mendez S, Shevach EM, Sacks DL. CD4+CD25+ regulatory T cells control Leishmania major persistence and immunity. Nature. 2002; 420:502–507. [PubMed: 12466842]
31. Lund JM, Hsing L, Pham TT, Rudensky AY. Coordination of early protective immunity to viral infection by regulatory T cells. Science. 2008; 320:1220–1224. [PubMed: 18436744]
32. Zelinskyy G, Dietze KK, Hüsecken YP, Schimmer S, Nair S, Werner T, Gibbert K, Kershaw O, Gruber AD, Sparwasser T, Dittmer U. The regulatory T-cell response during acute retroviral infection is locally defined and controls the magnitude and duration of the virus-specific cytotoxic T-cell response. Blood. 2009; 114:3199–3207. [PubMed: 19671923]
33. Thomas J, Gangappa S, Kanangat S, Rouse BT. On the essential involvement of neutrophils in the immunopathologic disease: herpetic stromal keratitis. J. Immunol. 1997; 158:1383–1391. [PubMed: 9013983]
34. Tumpey TM, Chen SH, Oakes JE, Lausch RN. Neutrophil-mediated suppression of virus replication after herpes simplex virus type 1 infection of the murine cornea. J. Virol. 1996; 70:898–904. [PubMed: 8551629]
35. Shevach EM. Mechanisms of foxp3+ T regulatory cell-mediated suppression. Immunity. 2009; 30:636–645. [PubMed: 19464986]
36. Masteller EL, Tang Q, Bluestone JA. Antigen-specific regulatory T cells--ex vivo expansion and therapeutic potential. Semin. Immunol. 2006; 18:103–110. [PubMed: 16458533]
37. Collison LW, Workman CJ, Kuo TT, Boyd K, Wang Y, Vignali KM, Cross R, Sehy D, Blumberg RS, Vignali DA. The inhibitory cytokine IL-35 contributes to regulatory T-cell function. Nature. 2007; 450:566–569. [PubMed: 18033300]

38. Zhao ZS, Granucci F, Yeh L, Schaffer PA, Cantor H. Molecular mimicry by herpes simplex virus-type 1: autoimmune disease after viral infection. Science. 1998; 279:1344–1347. [PubMed: 9478893]

39. Boyman O, Surh CD, Sprent J. Potential use of IL-2/anti-IL-2 antibody immune complexes for the treatment of cancer and autoimmune disease. Expert Opin. Biol. Ther. 2006; 6:1323–1331. [PubMed: 17223740]

40. Boyman O, Krieg C, Letourneau S, Webster K, Surh CD, Sprent J. Selectively expanding subsets of T cells in mice by injection of interleukin-2/antibody complexes: implications for transplantation tolerance. Transplant Proc. 2012; 44:1032–1034. [PubMed: 22564618]

41. Schreiber TH, Wolf D, Podack ER. The role of TNFRSF25:TNFSF15 in disease... and health? Adv. Exp. Med. Biol. 2011; 691:289–298. [PubMed: 21153333]

42. Reddy PB, Schreiber TH, Rajasagi NK, Suryawanshi A, Mulik S, Veiga-Parga T, Niki T, Hirashima M, Podack ER, Rouse BT. TNFRSF25 agonistic antibody and galectin-9 combination therapy controls herpes simplex virus-induced immunoinflammatory lesions. J. Virol. 2012

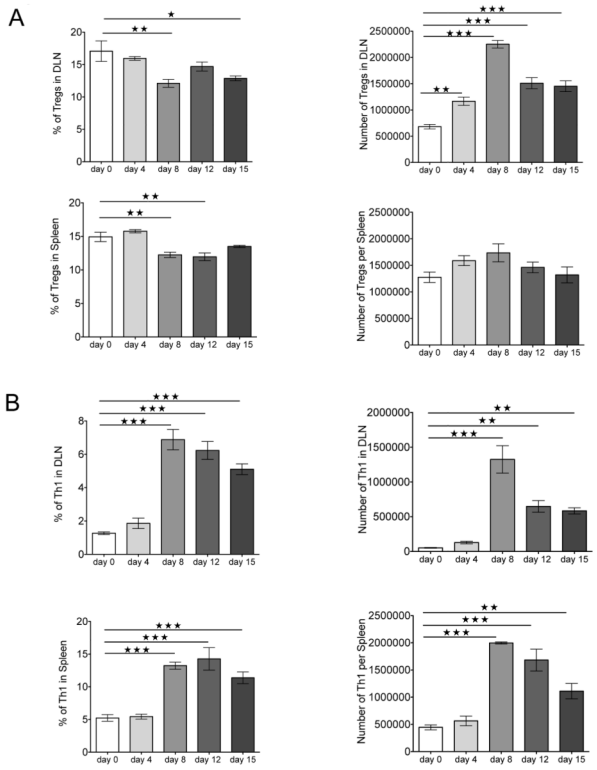

FIGURE 1.

Lymphoid Treg and Th1 response changes after HSV-1 infection. Foxp3^{-} GFP mice corneas were scarified and infected with HSV-1, and flow cytometry was used to quantify Treg and Th1 cells in DLN and spleen of naïve and infected mice at different times after corneal infection with HSV-1. (**A**) Representative frequencies and numbers of Treg in DLN and spleen of infected mice at different time points. (**B**) Representative frequencies and numbers of Th1 cells in DLN and spleen of infected mice at different times. Data are representative of three independent experiments and show mean values ± SEM (n = 6 mice at each indicated time point p.i.). ***$p \leq 0.001$,**$p \leq 0.01$,*$p \leq 0.05$. Statistical levels of significance were analyzed by one-way ANOVA test with Dunnett's post hoc test settings.

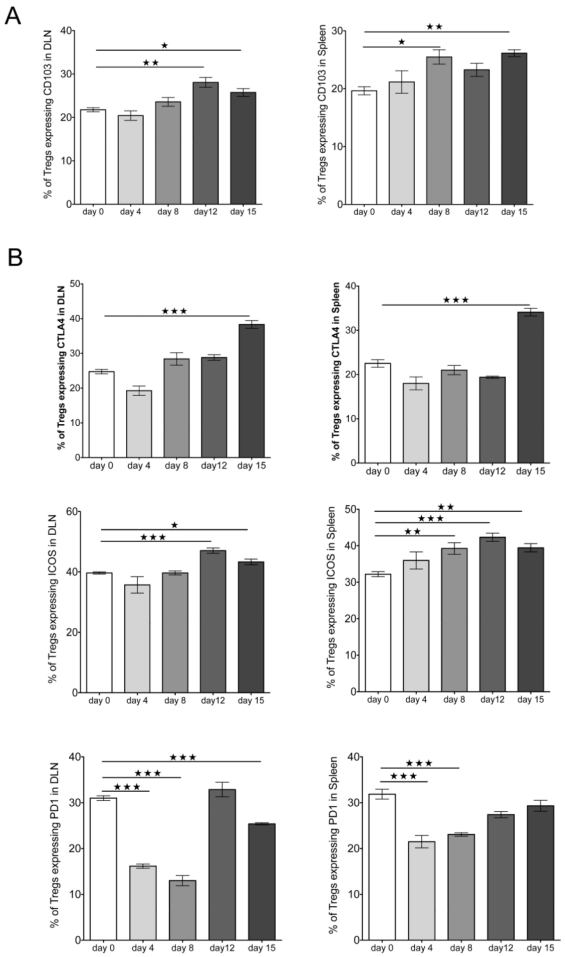

FIGURE 2.

HSV-1 infection changes Treg cell surface phenotype. Foxp3-GFP mice corneas were scarified and infected with HSV-1. (**A**) Flow cytometry was used to detect CD103 expression on Treg. Cells from DLN and spleen of naïve (day 0) and HSV-1-infected mice at different time points were stained for CD4 and CD103. Histograms were gated on $CD4^{+}Foxp3^{-}GFP^{+}$ cells. The frequencies of Treg expressing CD103 are shown. (**B**) Flow cytometry was used to detect different surface markers on Treg: CTLA-4, ICOS, and PD-1. Cells from DLN and spleen of naïve (day 0) and HSV-1-infected mice at different time points were stained for CD4, CTLA-4, ICOS, and PD-1. Histograms are gated on $CD4^{+}Foxp3\text{-}GFP^{+}$ cells. The frequencies of Treg expressing CTLA-4, ICOS, and PD-1 are shown. Data are representative of three independent experiments and show mean values ± SEM (n = 6 mice at each indicated time point p.i.). $^{***}p \leq 0.001$,$^{**}p \leq 0.01$(),$^{*}p \leq 0.05$. Statistical levels of significance were analyzed by one-way ANOVA test with Dunnett's post hoc test settings.

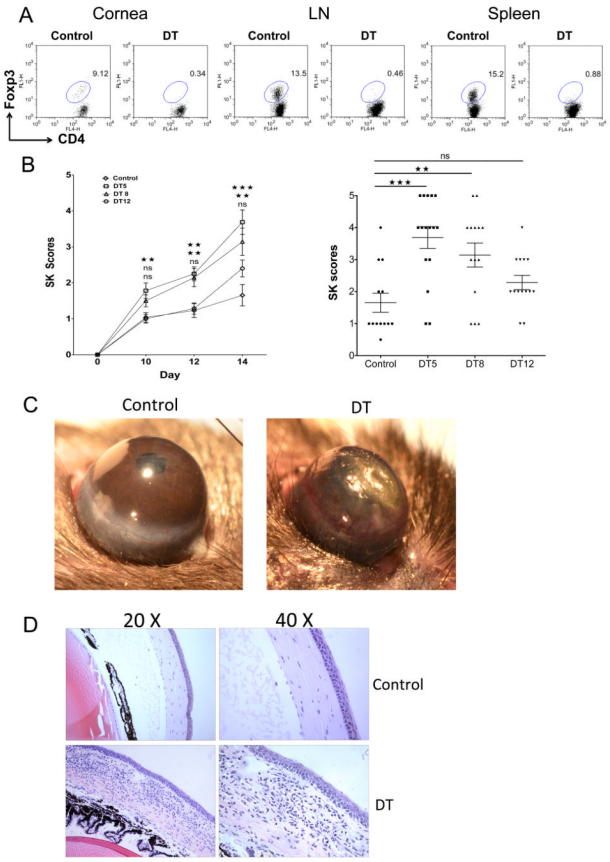

FIGURE 3.

Depletion of Treg during clinical stages of disease increases SK lesion severity. DEREG mice infected with HSV-1 were given either DT or vehicle IP starting on day 5 or 8 or 12 p.i., and treated every other day until the termination day (day 15 p.i.). (**A**) Starting on day 8 p.i. mice were treated either with DT (1μg/day) or vehicle every other day, mice were sacrificed on day 15 p.i., and lymphoid organs were removed. Flow cytometry analysis of lymphoid cells from cornea, DLN, and spleen show efficient depletion of Treg in DT-treated DEREG mice compared with DT PBS-treated DEREG mice. (**B**) The progression of SK lesion severity was significantly increased in the group of mice treated with DT as compared with control mice. Kinetics of SK lesion severity are shown. Individual eye scores of SK lesion severity on day 15 p.i. are shown. SK lesion severity was significantly increased in the groups of mice treated with DT starting on day 5 and 8 p.i. as compared with control mice. (**C**) Representative eye photos show increased SK lesion severity, as well as angiogenesis, from DT-treated mice starting on day 8 p.i. compared with vehicle-treated mice. (**D**) Eyes were processed for cryo-sections on day 15 p.i. Hematoxylin and eosin staining was carried out on 6-μm sections, and pictures were taken at different microscope augmentations (20X and 40X magnification). Representative eye sections show increased cellular infiltration in DT-treated mice starting on day 8 p.i. when compared to vehicle-treated animals. Data are representative of three independent experiments and show mean values ± SEM (n = 12-15 mice/group).

***$p \leq 0.001$,**$p \leq 0.01$,*$p \leq 0.05$. Statistical levels of significance were analyzed by the Student *t* test (unpaired).

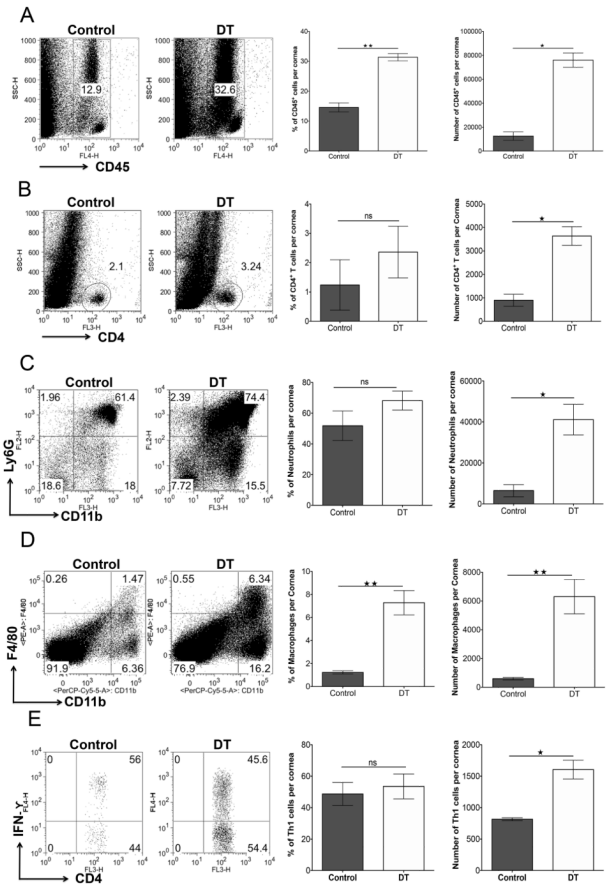

FIGURE 4.

Depletion of Treg increases cellular infiltration in corneas of HSV-1-infected animals. DEREG mice infected with HSV-1 were given either DT or vehicle IP starting on day 8 p.i. every other day until the termination day (day 15 p.i.). (**A**) Representative FACS plots, and frequencies and numbers of $CD45^+$ cells infiltrated in the corneas of control and DT-treated mice are shown. (**B**) Representative FACS plots, and frequencies and numbers of $CD4^+$ T cells infiltrated in the corneas of control and DT-treated mice. (**C**) Representative FACS plots, and frequencies and numbers of $CD11b^+$ $Ly6G^+$ polymorphonuclear neutrophils gated on total $CD45^+$ cells infiltrated in the corneas of control and DT-treated mice are shown. (**D**) Representative FACS plots, and frequencies and numbers of $CD11b^+$ $F4/80^+$ (macrophages) gated on total $CD45^+$ cells infiltrated in the corneas of control and DT-treated mice are shown. (**E**) Representative FACS plots, and frequencies and numbers of IFN-γ-secreting cells gated on $CD4^+$ T cells infiltrated in the cornea on day 15 p.i. and stimulated with PMA/ionomycin for 4 h from control and DT-treated mice. Data are representative of three independent experiments and show mean values ± SEM (n = 10-12 mice/group, each sample is representative of 2 corneas). $***p \leq 0.001$,$**p \leq 0.01$,$*p \leq 0.05$. Statistical levels of significance were analyzed by the Student *t* test (unpaired).

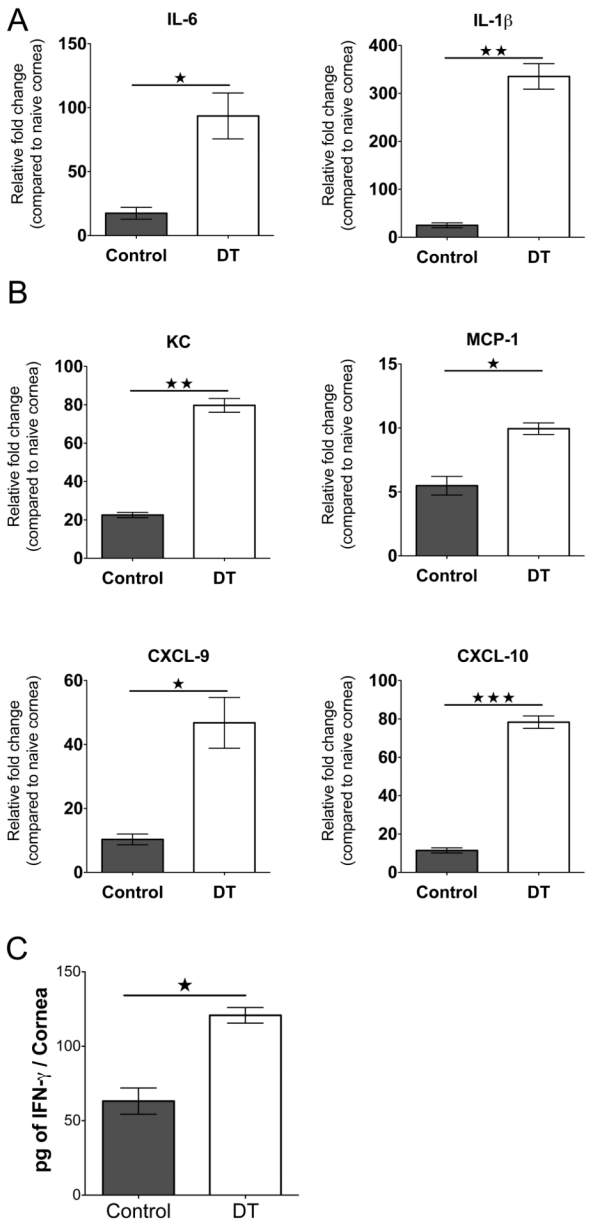

FIGURE 5.

Depletion of Treg increases cytokine and chemokine levels in corneas of HSV-1-infected animals. DEREG mice infected with HSV-1 were given either DT or vehicle i.p. starting on day 8 p.i. every other day until the termination day (day 15 p.i.). Mice were sacrificed on day 15 p.i., and corneal extracts were collected for measuring inflammatory factors using either Q-RT-PCR or sandwich ELISA. (**A**) Relative fold change in mRNA expression of the proinflammatory cytokines IL-1β and IL-6 was examined and compared between control and DT-treated mice on day 15 p.i. by Q-RT-PCR. (**B**) Relative fold change in mRNA expression of the chemokines KC, MCP-1, CXCL9, and CXCL10 was examined and compared between control and DT-treated mice on day 15 p.i. by Q-RT-PCR. mRNA levels for the different cytokines in mock-infected mice were set to one and used for the relative fold upregulation. (**C**) IFN-γ protein levels from pooled corneal samples from control and DT-treated animals were quantified using ELISA. Data are representative of three

independent experiments and show mean values ± SEM (n = 12 mice/group, each sample is representative of 4 corneas). ***$p \leq 0.001$,**$P \leq 0.01$,*$P \leq 0.05$. Statistical levels of significance were analyzed by the Student *t* test (unpaired).

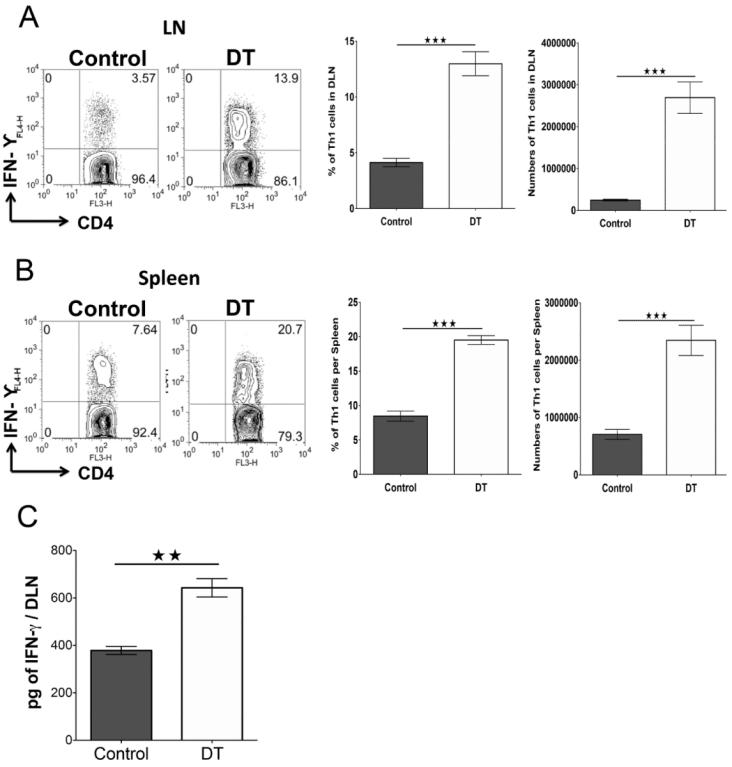

FIGURE 6.

Treg depletion increases Th1 responses and cell numbers in response to HSV-1 infection. DEREG mice infected with HSV-1 were given either DT or vehicle i.p. starting on day 8 p.i. every other day until the termination day (day 15 p.i.). (**A**) Representative FACS plots, and frequencies and numbers of IFN-γ-secreting cells gated on $CD4^+$ T cells infiltrated in DLN on day 15 p.i. and stimulated with PMA/ionomycin for 4 h from control and DT-treated mice. (**B**) Representative FACS plots, and frequencies and numbers of IFN-γ-secreting $CD4^+$ T cells from spleen on day 15 p.i. from control and DT-treated mice. (**C**) IFN-γ protein levels analyzed by ELISA from control and DT-treated DLN and spleen on day 15p.i. Data are representative of three independent experiments and show mean values ± SEM (n = 10-12 mice/group). $^{***}p \leq 0.001$,$^{**}p \leq 0.01$,$^{*}p \leq 0.05$. Statistical levels of significance were analyzed by the Student *t* test (unpaired).

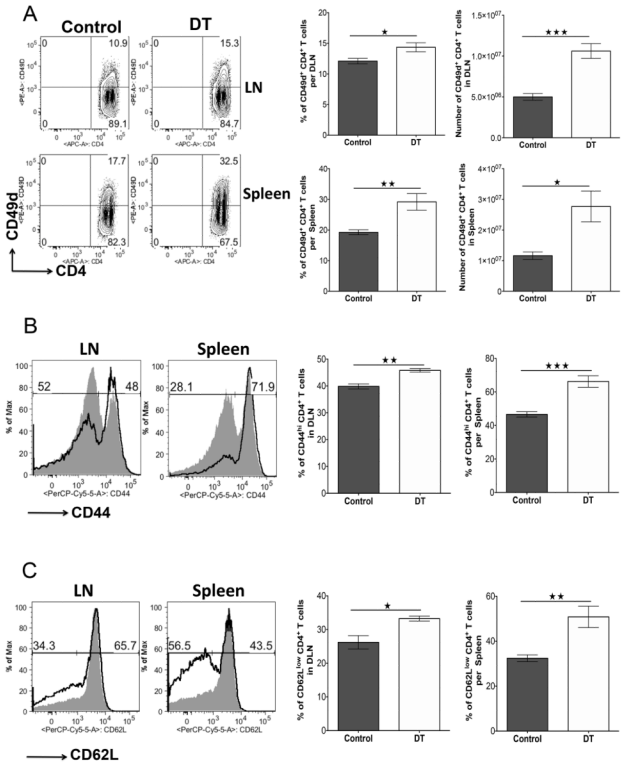

FIGURE 7.

Treg depletion during the clinical phase of SK causes phenotype changes in secondary lymphoid tissue effectors. DEREG mice infected with HSV-1 were given either DT or vehicle IP starting on day 8 p.i. every other day until the termination day (day 10 p.i.). (**A**) Representative FACS plots, and frequencies and numbers of $CD4^+CD49d^+$ T cells in DLN and spleen of control and DT-treated mice are shown. (**B**) Representative histogram plots and frequencies of $CD4^+CD44^{hi}$ T cells in DLN and spleen of control (gray) and DT-treated (thick line) mice are shown. (**C**) Representative histogram plots and frequencies of $CD4^+CD62L^{low}$ T cells in DLN and spleen of control (gray) and DT-treated (thick line) mice are shown. Data are representative of three independent experiments and show mean values ± SEM (n = 10-12 mice/group). $^{***}p \leq 0.001$,$^{**}p \leq 0.01$,$^{*}p \leq 0.05$. Statistical levels of significance were analyzed by the Student *t* test (unpaired).